Synthesis and characterization of nanoscale dendritic RGD clusters for potential applications in tissue engineering and drug delivery

Hu Yang[1]
Weiyuan John Kao[2,3]

[1]Department of Biomedical Engineering, School of Engineering, Virginia Commonwealth University, Richmond, VA, USA; [2]School of Pharmacy, University of Wisconsin-Madison, Madison, WI, USA; [3]Department of Biomedical Engineering, College of Engineering, University of Wisconsin-Madison, Madison, WI, USA

Abstract: Spatial control over the distribution and the aggregation of arginine-glycine-aspartate (RGD) peptides at the nanoscale significantly affects cell responses. For example, nanoscale clustering of RGD peptides can induce integrins to cluster, thus triggering complete cell signaling. Dendrimers have a unique, highly branched, nearly spherical and symmetrical structure with low polydispersity, nanoscale size, and high functionality. Therefore, dendrimers are a class of ideal scaffold for construction of nanoscale dendritic RGD clusters in which RGD loading degree and cluster size can be finely adjusted. This new type of nanoscale dendritic RGD cluster will aid us to better understand the impact of spatial arrangement of RGD on cellular responses and to engineer RGD to trigger more favorable cellular responses. In this study, nanoscale dendritic RGD clusters were synthesized based on Starburst™ anionic G3.5 and cationic G4.0 polyamidoamine (PAMAM) dendrimers. The multiple terminal functional groups on the outermost layer of the dendrimer were coupled with RGD tripeptides. Biofunctionalized dendrimer structures were found to be highly dependent on the generation and the extent of peptide modification (ie, number of peptides per PAMAM dendrimer). Fluorescein isothiocyanate (FITC)-conjugated PAMAM dendrimers were utilized to monitor cellular internalization of dendrimers by adherent fibroblasts. Anionic G3.5-based dendritic RGD clusters have been shown to have no negative effect on fibroblast viability and a concentration-dependent effect on lowering cell adhesion on tissue culture polystyrene (TCPS) as that of free RGD. A similar concentration-dependent effect in cell viability and adhesion was also observed for cationic G4.0-based dendritic RGD clusters at lower but not at high concentrations. The results imply that the synthesized nanoscale dendritic RGD clusters have great potential for tissue engineering and drug delivery applications.

Keywords: biofunctionalized dendrimer, confocal image, cytocompatibility, dendritic peptide, nanoclusters

Introduction

The arginine-glycine-aspartate (RGD) sequence present in many extracellular matrix (ECM) proteins such as collagen, fibronectin, laminin, and vitronectin has been identified as a cell recognition motif to stimulate integrin-mediated cell adhesion (Ruoslahti and Pierschbacher 1987). Similar to the RGD sequence in ECM proteins, synthetic peptides containing the RGD sequence can promote cell adhesion after being immobilized on a surface (Kao 1999). Therefore, polymers modified with RGD as bioactive materials have been employed in a variety of tissue engineering and drug delivery applications. RGD spatial distribution patterns, as well as RGD concentration, affect cell adhesion, migration, and proliferation. It has been noticed that nanoscale clustering of RGD peptides plays an important role in regulating cellular responses. For example, RGD nanoclusters could better trigger cell adhesion by inducing integrin receptors to cluster in the cell membrane (Burridge et al 1988; Shaw et al 1990; Kornberg et al 1991; Ginsberg et al 1992; Miyamoto, Akiyama, et al 1995; Miyamoto, Teramoto,

Correspondence: Hu Yang
Department of Biomedical Engineering, Virginia Commonwealth University, 701 West Grace Street, Richmond, VA 23284, USA
Tel +1 804 828 5459
Fax +1 804 827 0290
Email hyang2@vcu.edu

© 2007 Dove Medical Press Limited. All rights reserved

et al 1995). Maheshwari and colleagues (2000) demonstrated that cell motility could be adjusted by varying RGD ligand spatial arrangement at the nanoscale level and suggested that integrin clustering should be required to support cell motility. Irvine and colleagues (2001) employed comb copolymers of methyl methacrylate and poly (oxyethylene) methacrylate to construct nanoclusters of RGD peptides and achieved tunable control over cell adhesion (Irvine, Mayes, et al 2001; Irvine, Ruzette, et al 2001).

Nanoclustering of RGD not only can serve as a unique matrix to elicit integrin-mediated cell responses but also has great potential for tissue engineering and drug delivery applications. Dendrimers are a new class of polymers playing an important role in the emerging filed of nanobiotechnology (Bosman et al 1999; Yang and Kao 2006). Different from traditional polymers, dendrimers have a highly branched, three-dimensional, nanoscale architecture with very low polydispersity and high functionality (Tomalia et al 1985). Applications of dendrimers have been explored for drug delivery (Poxon et al 1996; Yang et al 2004; Yang and Lopina 2005, 2006), gene transfer (Bielinska et al 2000; Eichman et al 2000; Luo et al 2002), imaging of biological systems (Kobayashi et al 2001; Bielinska et al 2002), etc. As dendrimers have controllable structural components, including type and number of surface groups, surface charge, and scaffold size, they are a class of ideal scaffold for construction of nanoscale dendritic RGD clusters in which RGD loading degree and cluster size can be finely adjusted. This new type of nanoscale dendritic RGD cluster with finely controllable structural components will help us to better understand the impact of spatial arrangement of RGD on cellular responses and to engineer RGD to trigger more favorable cellular responses, eg, rapid and stable cell adhesion. In this study, Starburst™ polyamidoamine (PAMAM) dendrimers were applied to construct nanoscale dendritic RGD clusters. The diameter of a PAMAM dendrimer molecule ranges from approximately 1.5 nm for G0 to 14.5 nm for G10. The primary amine or carboxylate surface groups on the outermost layer of the PAMAM dendrimer could be modified to covalently link with RGD-containing peptides. Shukla and colleagues (2005) provided the first dendrimer-RGD example by coupling bicyclic CDCRGDCFC (RGD-4C) to G5.0 PAMAM dendrimer for potential targeted cancer therapy. Nevertheless, the use of low generation dendrimers is preferred because low generation PAMAM dendrimers (below G5.0) have been shown to be potentially more biocompatible and less immunogenic than high generation PAMAM dendrimers. To demonstrate the feasibility of using low generation PAMAM dendrimers as RGD carrier, G3.5 and G4.0 PAMAM dendrimers and the tripeptide RGD sequence, ie, Arg-Gly-Asp, were used as the underlying materials to synthesize RGD clusters. G3.5 and G4.0 PAMAM dendrimers contain 64 carboxylate and 64 primary amine surface groups, respectively, to which the N-terminus of the RGD tripeptide was conjugated. As the RGD tripeptide has the simplest structure and the lowest steric hindrance among the RGD-containing peptides, high RGD loading degrees could be achieved. To prove the robustness of the synthetic methods presented here, triglycine (gly-gly-gly or GGG) was used as another tripeptide model and conjugated to G3.5 and G4.0 following the same synthetic strategies. A series of G3.5- and G4.0-based nanoscale dendritic tripeptide clusters were synthesized and characterized with gel permeation chromatography (GPC) and proton nuclear magnetic resonance (^{1}H-NMR) spectroscopy. The cytotoxicity of dendrimers after being modified with tripeptides was evaluated using fibroblasts. In addition, the effect of dendritic RGD peptides on fibroblast adhesion to tissue culture polystyrene (TCPS) was investigated and discussed.

Materials and methods

Materials

Starburst™ G3.5 and G4.0 PAMAM dendrimers, triglycine (GGG), 1-ethyl-3-(3-dimethylaminopropyl) carbodiimide hydrochloride (EDC), N,N'-disuccinimidyl carbonate (DSC), N-hydroxysuccinimide (NHS), dimethylformamide (DMF), FITC, triethylamine (TEA), and sodium bicarbonate ($NaHCO_3$) were purchased from Sigma-Aldrich (St. Louis, MO) and used as received. RGD was obtained from the Biotechnology Center of University of Wisconsin-Madison. The purity of RGD was over 95% as analyzed with high performance liquid chromatography (HPLC) and matrix-assisted laser desorption/ionization time-of-flight (MALDI-TOF) A cell counting kit-8 (CCK-8) for cell viability tests was purchased from Dojindo (Kumamoto, Japan). BioCoat™ poly-D-lycine coverslip bottom-dishes were purchased from BD Biosciences (San Jose, CA). Milli-Q deionized water was used throughout the studies.

Characterization

^{1}H-NMR spectra were acquired and processed on a 400 MHz Varian ^{UNITY}INOVA spectrometer (Palo Alto, CA). The internal reference standard was tetramethylsilane

(TMS). Deuterium oxide (D_2O, 99.9%) was obtained from Cambridge Isotope Laboratories (Andover, MA). Each sample was dissolved in D_2O, filtered, and degassed before measurement. The chemical shift for D_2O is 4.8 ppm.

GPC analyses were performed on a Waters Breeze™ GPC system (Milford, MA). The GPC system contained three Ultrahydrogel™ columns – Ultrahydrogel™ Linear, Ultrahydrogel™ 1000, and Ultrahydrogel™ 250 – to cover the molecular weight ranging from 1×10^3 to 7×10^6 daltons. The mobile phase was composed of 80 wt% 0.1 M $NaNO_3$ and 20 wt% acetonitrile. The eluent with a flow rate at 0.5 mL/min was monitored by a Waters 2414 refractive index detector.

Synthesis of dendritic tripeptide nanoclusters

G3.5-based dendritic peptides

Before being coupled with RGD, the carboxylate surface groups of G3.5 were converted to active NHS esters, following the method described previously (Yang and Lopina 2003, 2005) (Scheme 1). Briefly, 30 mg of dry G3.5 was obtained after removal of methanol from the storage solution using rotary evaporation. The desiccated G3.5 sample was then dissolved in 2 mL of deionized water and acidified to pH 3 or below with a few drops of 1 N hydrochloric acid. The acidified G3.5 was evaporated to dryness under vacuum, and then redissolved in a mixture solution containing 0.8 mL of DMF and 0.2 mL of deionized water. To the G3.5 solution were added 22.7 mg of NHS and 39.4 mg of EDC. NHS-activated G3.5 was then produced after 14 h reaction. Following a vacuum drying step, the NHS-activated G3.5 continued to react with RGD in 2 mL of pH 8.5 sodium bicarbonate solution for 2 h where the feeding molar ratio of RGD/G3.5 was 64:1. After extensive dialysis and subsequent lyophilization, RGD-G3.5 was obtained and characterized with GPC and ^{1}H-NMR. A series of GGG-G3.5 were synthesized by varying the feeding molar ratio of GGG/G3.5 (16:1, 32:1, and 64:1) following the same synthesis procedures as described above.

G4.0-based dendritic peptides

Similar to the synthesis of G3.5-based dendritic peptides, the primary amine surface groups of G4.0 were converted to active NHS esters first (Scheme 2). Briefly, 1.8 mL of DMF containing 30 mg of G4.0 was dropwise added to a DMF solution (2 mL) containing 35 mg of DSC. Afterwards, slow addition of TEA to the solution was performed and then followed by an overnight reaction with stirring. The supernatant containing NHS-activated G4.0 was collected after centrifugation. The NHS-activated G4.0 was then precipitated out of cold ether and vacuum dried. A 2-h coupling reaction between NHS-G4.0 and RGD was carried out in a pH 8.5 biocarbonate buffer solution where the feeding molar ratio of RGD/G4.0 was 64:1. The resulting RGD-G4.0 was purified by using extensive dialysis and then characterized with GPC and ^{1}H-NMR. A series of GGG-G4.0 with various feeding ratio of GGG/G4.0 (16:1, 32:1, and 64:1) were obtained using the above synthesis procedures.

Cytotoxicity assay

The potential cytotoxic effect of the synthesized dendritic tripeptides was investigated in vitro using fibroblasts. Clonetics™ dermal fibroblast systems were purchased from Cambrex (Walkersville, MD). The systems contained normal human dermal fibroblasts and cell growth medium, ie, Clonetics FGM® BulletKit. The BulletKit contained fibroblast cell basal medium and growth supplements: hFGF-B, insulin, and GA-1000. Cell culture of fibroblasts followed the protocols provided by the supplier.

The wells of 96-well plates were plated with 2000 fibroblasts in 100 μL of growth medium. Fibroblasts were then allowed to adhere and grow for two days at 37 °C in an atmosphere of 5% CO_2 and 95% relative humidity. The cells were then exposed to 0.2, 2, or 20 μM of G3.5, G4.0, or dendritic triglycine in medium for 12, 24, or 96 h. At the end of each predetermined time point, the treated cells were assayed using a CCK-8 kit, where 10 μl of CCK-8 solution was added to 100 μL of fresh growth medium. Two hours later, the optical absorbance of medium in each well was read

Scheme 1 Synthesis of RGD-G3.5 conjugates.
Abbreviation: RGD, arginine-glycine-aspartate..

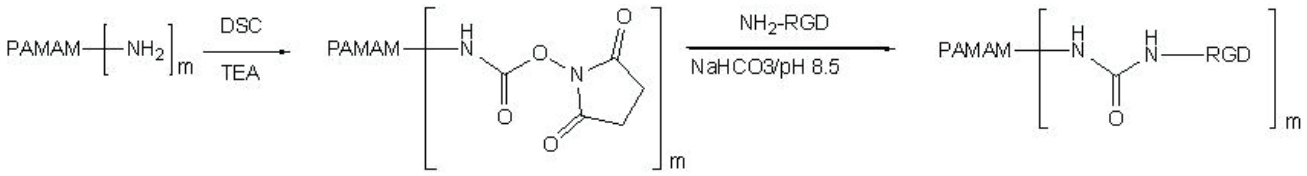

Scheme 2 Synthesis of RGD-G4.0 conjugates.
Abbreviation: RGD, arginine-glycine-aspartate.

on an EL × 800™ absorbance microplate reader (Bio-TEK) at a test wavelength of 450 nm and a reference wavelength of 630 nm. Cell viability was calculated as follows:

$$\text{Cell viability (\%)} = \frac{A_{test} - A_{blank}}{A_{control} - A_{blank}} \times 100$$

where A_{test} is absorbance of a well with cells, CCK-8 solution and polymer solution; A_{blank} is absorbance of a well with medium and CCK-8 solution, without cells; $A_{control}$ is absorbance of a well with cells and CCK-8 solution, without polymer solution. Morphology of fibroblasts was observed on an Olympus TE300 phase-contrast microscope at a total 100 × magnification. The cell viability data were expressed as means ± SEM (n = 4). In order to take account of the potential cytotoxic effect of RGD-dendrimer on cell adhesion, fibroblasts were exposed to 0.77, 77, or 770 μM of free RGD, RGD-G3.5 or RGD-4.0 for 2 h. The cell viability at 2, 24, and 96 h post treatment was determined using the same method as described above.

Cellular entry of FITC-labeled G4.0 PAMAM dendrimer

To label G4.0 PAMAM dendrimer with FITC, the corresponding amount of FITC (dendrimer/FITC molar ratio=1:1) was dissolved in acetone to give a solution of concentration <5 mg/ml and then added to the pH 7.4 PBS solution where G4.0 was dissolved previously. The FITC/G4.0 was thoroughly mixed overnight at room temperature with stirring. The FITC-labeled G4.0 solution was then dialyzed against deionized water to remove the unconjugated FITC. The resulting FITC-G4.0 conjugates were subsequently lyophilized and stored at 4 °C when not in use. Fibroblasts were plated on the poly-D-lysine coated glass bottom culture dishes at the seeding density of 1×10^4 cells/mL. Two days later, FITC-G4.0 conjugates were added to the cell medium at the final concentration of 0.422 mg/mL and allowed to interact with fibroblasts for 15 min, 1 h, and 2 h, respectively. By the end of each predetermined time point, the old growth medium was removed and the cells were rinsed three times with fresh growth medium. The cells were then imaged with a Radiance 2100-multiphoton/confocal imaging (Bio-Rad) system. The cells were visualized vertically at different sections with 2 μm thickness between two neighbor sections. The overall magnification was 400 ×.

Fibroblast adhesion to TCPS in dendritic peptide suspension

Freshly isolated fibroblasts at 10^4 cells/mL in 100 μL of serum-free medium were transferred to each well of a TCPS 96-well culture plate and exposed to 0, 0.77, 77, or 770 μM of free RGD, RGD-G3.5, or RGD-G4.0 for 2 h. After the unattached fibroblasts were aspirated out, adherent fibroblasts at 2 h and 96 h post treatment were quantified based on measurements from three randomly selected fields using an Olympus TE300 phase-contrast microscope.

Statistical analysis

The data were expressed as means ± SEM. Statistical evaluation of the data was performed by analysis of variance (ANOVA) followed by Student-Newman-Keuls test for pairwise comparison of subgroups. Differences among means were considered statistically significant at a p value of ≤0.05.

Results and discussion

Cytotoxicity of dendritic peptides

Nanoscale dendritic clusters of RGD and GGG tripeptides were synthesized and analyzed in a similar way owing to the similarity in their chemical structures. As the C-terminus of RGD is essential for keeping RGD active in mediating integrin-based cell adhesion, the N-terminus of the RGD tripeptide was modified to link with the ending groups on the dendrimer surface (Hersel et al 2003). NHS-activated esters can readily react with the primary amine group present at the N-terminus of the peptide. To achieve high peptide loading degree, dendrimer surface groups were converted

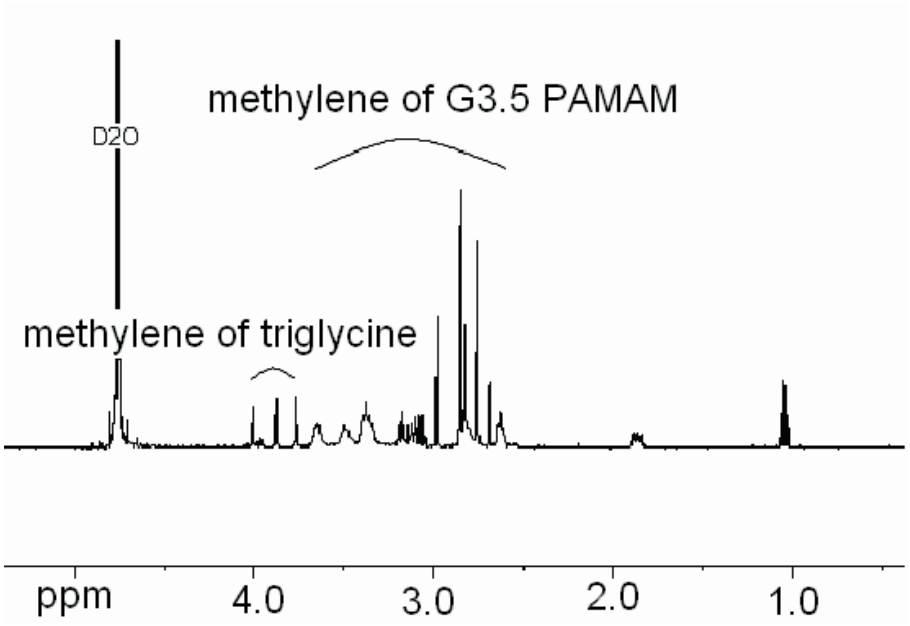

Figure 1 ^{1}H-NMR spectrum of 16GGG-G3.5.
Abbreviations: ^{1}H-NMR, proton nuclear magnetic resonance.

to active NHS-activated esters prior to the coupling reaction. NHS and DSC were used to activate carboxylate and primary amine surface groups, respectively. The resulting dendritic tripeptides were then characterized with GPC and ^{1}H-NMR. According to the GPC data, dendritic clusters of tripeptides showed distinct peak domains based on elution time as peptide loading degree varied. ^{1}H-NMR spectroscopy was applied to further analyze the structure of the tripeptide-dendrimer conjugates. For example, the ^{1}H-NMR spectrum of 16GGG-G3.5 (Figure 1) shows the presence of the proton peaks of both GGG (three methylene peaks between 3.75 ppm and 4.00 ppm) and G3.5 (multiple methylene protons between 2.5 ppm and 3.6 ppm), indicating the success of coupling of GGG to G3.5. Peptide loading degree depends on the feeding ratio of peptide/dendrimer, reaction conditions, and coupling efficiency (Yang et al 2004).The peptide loading degree was estimated between 80%–90% according to the ^{1}H-NMR spectrum. High peptide loading degrees were achieved because of activation of the surface groups by NHS and the negligible steric hindrance of RGD and GGG.

It has been well recognized that the cytotoxicity of dendrimers is a function of surface charge, size, and concentration (Jevprasesphant et al 2003). The interaction between positively charged dendrimers and negatively charged cell surfaces is believed to be the cause of the cytotoxicity of cationic PAMAM dendrimers that contain primary amine surface groups. Surface modification has proved to be an effective way to minimize the cytotoxicity of dendrimers by decreasing the overall positive surface charge of the dendrimer (Roberts et al 1996; Malik et al 2000; Jevprasesphant et al 2003). The effect of tripeptide conjugation on the cytotoxicity of the dendrimer was investigated using fibroblasts. The cytotoxicity assay (CCK-8 kit) measured the activity of most of the dehydrogenases in a fibroblast cell. As shown in Figure 2A, G3.5 PAMAM dendrimer did not induce a cytotoxic response in fibroblasts at 0.2, 2, or 20 μM for up to 96 h. Furthermore, GGG-modified G3.5 PAMAM did not induce cytotoxicity to fibroblasts (Figure 2B, C, and D). All data points were statistically comparable. The cytotoxicity of G4.0 PAMAM dendrimer was concentration and time dependent. G4.0 PAMAM dendrimer did not cause fibroblast viability loss at 0.2 μM up to 96 h; however, G4.0 PAMAM dendrimer significantly reduced the cell viability as the concentration and incubation time increased. There were no viable fibroblasts after 96 h-incubation when the concentration of G4.0 was 2 μM or 20 μM (Figure 3A). Coupling of GGG to the dendrimer surface significantly reduced the cytotoxicity of G4.0, extending the toxicity tolerance of fibroblasts to the triglycine-modified G4.0 PAMAM dendrimers from 0.2 μM to 2 μM within 96 h (Figures 3B, 3C, and 3D). Among triglycine-loaded G4.0 PAMAM dendrimers, 64GGG-G4.0 showed remarkably high cytocompatibility even at 20 μM up to 12 h, which was comparable to that at 0.2 and 2 μM. In addition, 64GGG-G4.0 appeared to have

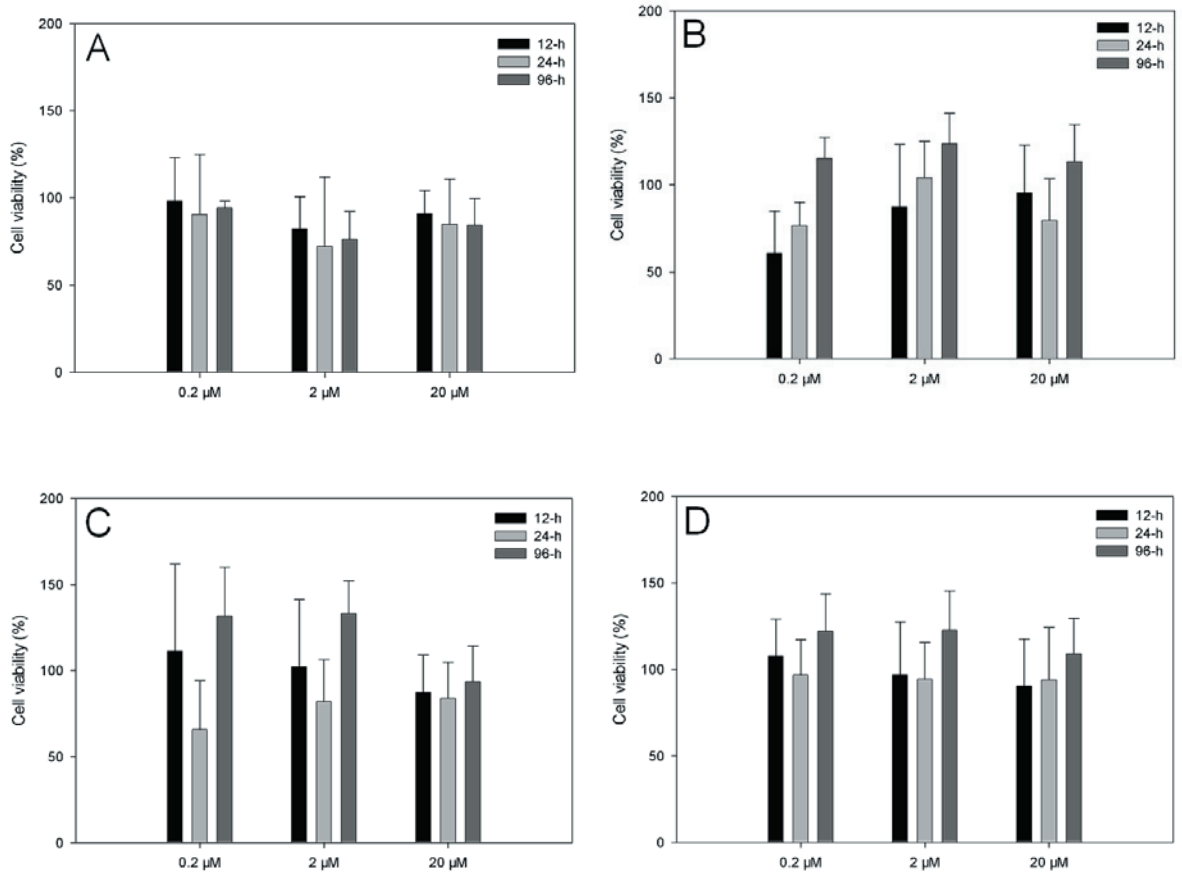

Figure 2 Viability of fibroblasts incubated with G3.5 (A), 16GGG-G3.5 (B), 32GGG-G3.5 (C), and 64GGG-G3.5 (D).

had little effect on the fibroblast cell morphology compared with the control cells at 12 h.

Through the modification with GGG, the cytotoxicity of G4.0 PAMAM dendrimer was reduced significantly. However, the cytotoxicity reduction of G4.0 depended on peptide loading degree, and the toxicity tolerance of fibroblasts to peptide-loaded G4.0 was time and concentration dependent. Cell morphology was consistent with cell viability changes. The cells without cytotoxic effect spread over; in contrast, the cells with cytotoxic effect became rounded and started to die. As shown in Figure 4, at 20 μM, 64GGG-G4.0 has much less cytotoxic effect on cell morphology than 16GGG-G4.0 and 32GGG-G4.0 up to 24 h. The results indicated that the conjugation of tripeptides to the dendrimer surface resulted in reduction of cytotoxicity of cationic G4.0 PAMAM dendrimer.

Internalization of FITC-labeled cationic G4.0 by fibroblasts

The interaction between G4.0 PAMAM dendrimer with fibroblasts was visualized by coupling FITC to the dendrimer surface. The confocal images have shown that the FITC-labeled G4.0 could enter inside the fibroblast within 15 min (Figure 5A-D). The staining at 15 min is punctuated, suggesting that dendrimers were endocytosed following the endosome/lysosome pathway. The strong fluorescence signals were found throughout the cytoplasm at the later time points, indicating a major accumulation place of FITC-labeled G4.0 PAMAM dendrimer inside the fibroblast. This result was similar to the dendrimer localization within human lung carcinoma epithelial cell line A549 (Khandare et al 2005) and Caco-2 cells (Jevprasesphant et al 2004). In addition, the visualization of fluorescence at horizontal layers (from A to D) confirmed that FITC-G4.0 did enter the cell instead of attaching to the cell membrane. As shown in Figure 5, the very strong fluorescence signals at the edge of the cell suggest that a certain fraction of FITC-G4.0 molecules may still bind to the cell membrane due to the electrostatic interactions during the observation. The binding of fluorescein-labeled PAMAM dendrimers to the surface of individual fibroblast cells has been confirmed and quantified using

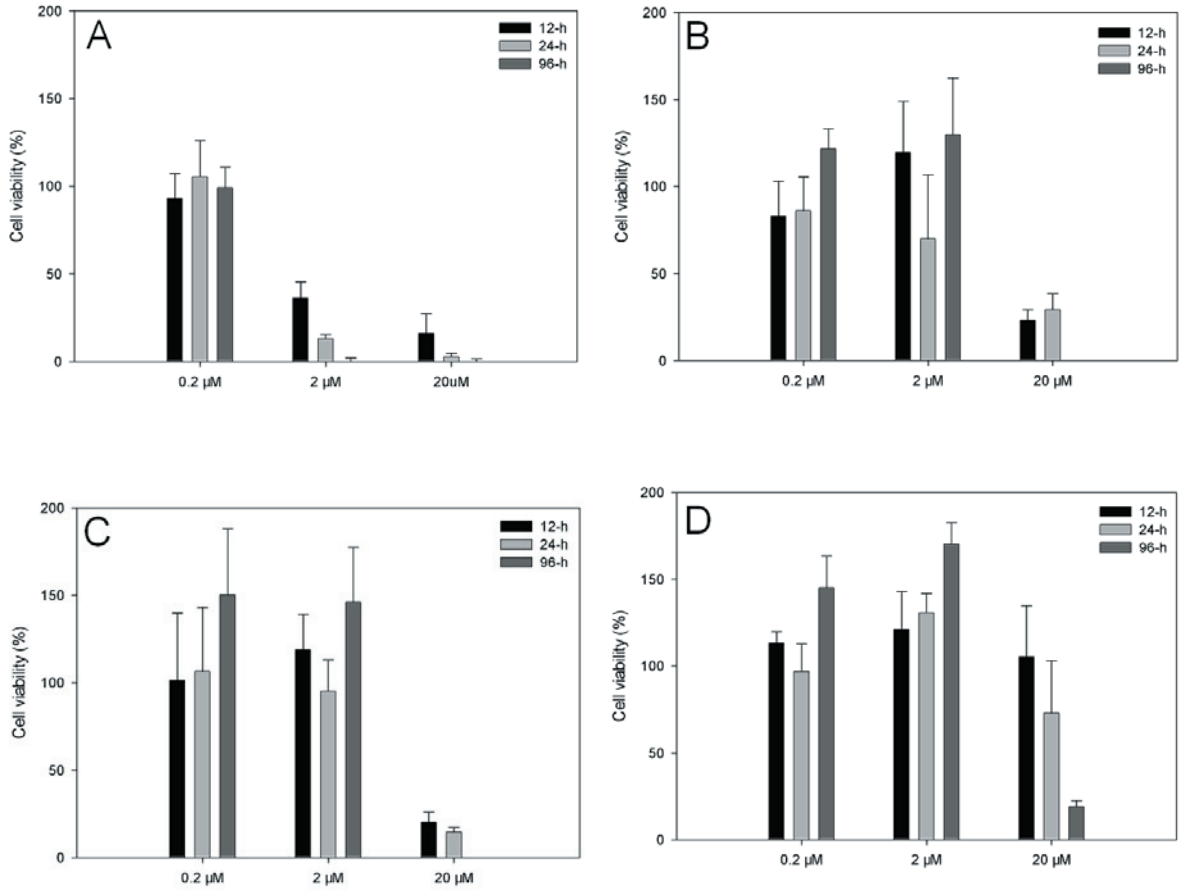

Figure 3 Viability of fibroblasts incubated with G4.0 (A), 16GGG-G4.0 (B), 32GGG-G4.0 (C), and 64GGG-G4.0 (D).

confocal fluorescence microscopy in a previous work done by Lai and colleagues (2002). The internalized FITC-G4.0 PAMAM dendrimers remained stably and intracellularly over 2 hours (Figure 5F). The nonspecific intracellular localization of FITC-G4.0 may cause many organelles to be involved with G4.0 PAMAM dendrimer. Particularly, the cell viability measured in this study was based on the cell's dehydrogenase activity. Mitochondria play an important role in regulating cell death and many dehydrogenases are found inside the mitochondrion. We hypothesized that the loss of cell viability may be due to the interference of the internalized G4.0 PAMAM dendrimers with mitochondria. However, more biological assays and measurements are needed to verify this hypothesis and beyond the focus of this study. Nevertheless, quick entry into cell membrane and intracellular stabilization has made cationic PAMAM dendrimers like G4.0 have strong cytotoxic effect on cell viability. It must be noted that these phenomena are reflective of the property of FITC-conjugated PAMAM and not PAMAM-only. The influence of FITC molecules in cellular uptake should also be considered.

Fibroblast adhesion to TCPS in dendritic peptide suspension

TCPS is a commonly used substrate to support cell attachment, spreading, and proliferation. To evaluate the bioavailability of RGD after being conjugated to the dendrimer, fibroblast adhesion to TCPS in the dendritic RGD suspension was quantified in terms of adherent cell density. Fibroblasts were treated with free RGD, RGD-3.5, and RGD-4.0 of varying concentrations in a serum-free medium for 2 h. After the unattached cells were gently rinsed out, the adherent fibroblasts on the TCPS were counted at 2 h and 96 h post treatment. By varying the concentration of free RGD in a wide range from 0.77 μM to 770 μM, free RGD inhibited cell adhesion on TCPS in a concentration-dependent manner. At 0.77 μM, the presence of free peptides had little effect on cell adhesion compared with the control cells. So

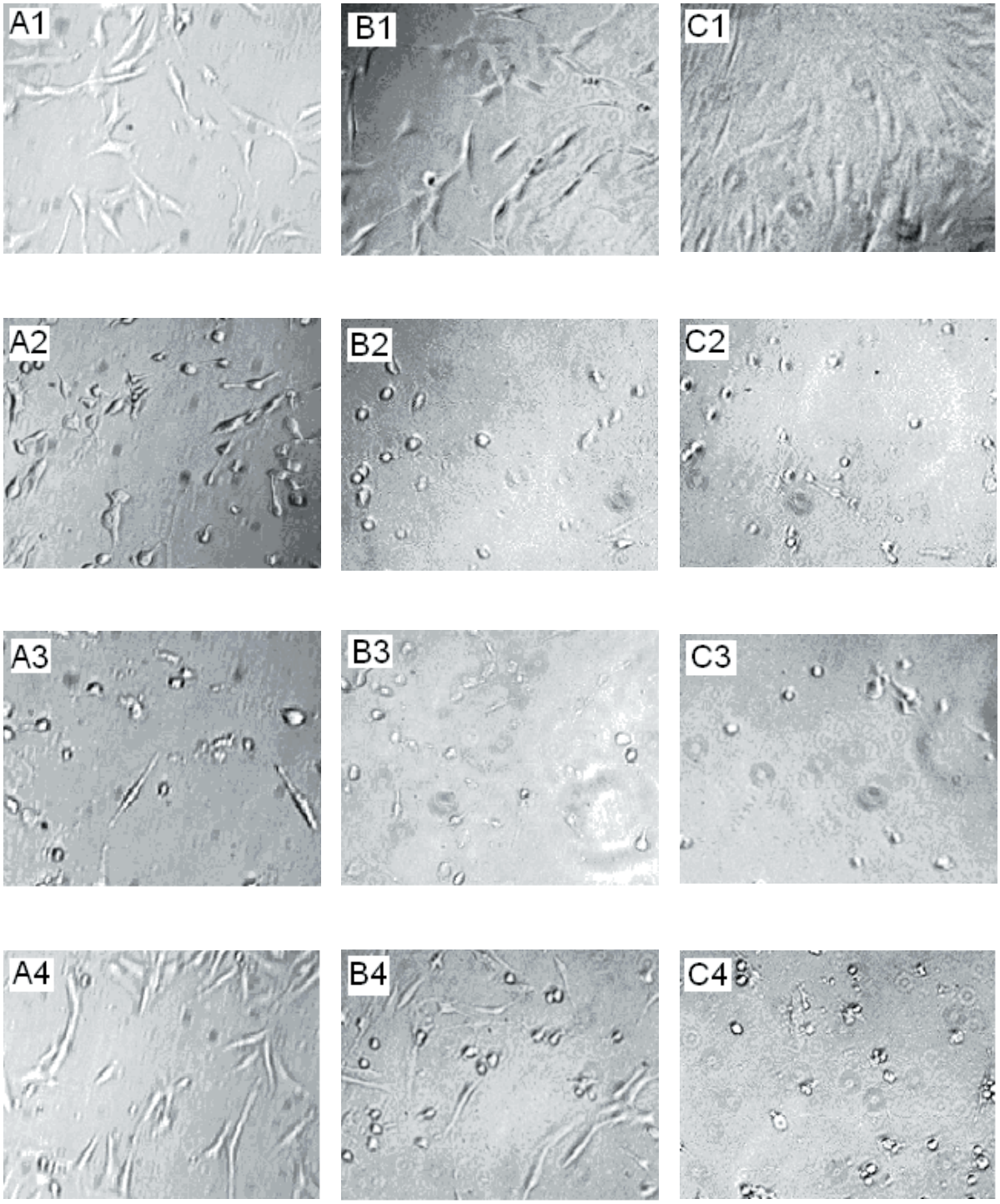

Figure 4 Morphology of fibroblasts incubated with 20 μM of GGG-G4.0 conjugates (A, 12 h; B, 24 h; C, 96 h; 1, control; 2, 16GGG-G4.0; 3, 32GGG-G4.0; 4, 64GGG-G4.0).

did RGD-3.5 and RGD-G4.0 at 0.77 μM. But, free RGD peptides decreased the number of adherent fibroblasts as the concentration increased (Figure 6). At 770 μM, RGD significantly inhibited cell adhesion. The cell density, after RGD treatment at 770 μM for 2 h, dropped 70%–75% compared with the control. To compare the dendritic RGD peptides with the RGD tripeptide, we chose to make the concentrations of dendritic peptides equivalent to those of free RGD peptides. We found the similar decrease in cell density as the concentration of dendritic peptides increased. The concentrations at 77 μM and 770 μM were much higher than the range we chose for the cytotoxicity study. Cytotoxicity

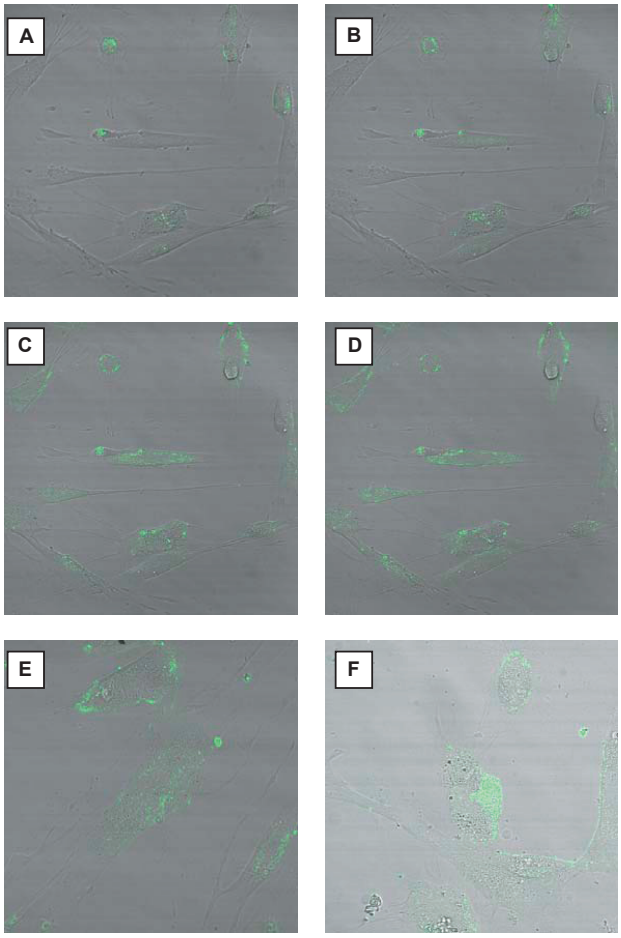

Figure 5 Confocal images of fibroblasts at different horizontal sections at 15 min (from A (apical) to D (basal), 2 μm thickness between two neighbor sections), 1 h (E), and 2 h (F) (magnification 400×).

induced by such high concentration doses may also cause cell adhesion inhibition. In order to consider the cytotoxic effect of dendritic peptides on fibroblast adhesion, cell viability at 2, 24, and 96 h post 2-h-treatment with dendritic peptides was measured using the CCK-8 kit. According to the cytotoxicity assay (Figure 7), RGD-G4.0 at 770 μM was most toxic, causing permanent damage to fibroblasts at 24 h and 96 h, which, however, was not obvious at 2 h. The cytotoxicity of RGD-G4.0 at 77 μM was mild, causing a 20% drop of cell viability. The decrease in adherent cell density at the presence of RGD-G4.0 was mainly due to RGD-G4.0 cytotoxicity. Like free RGD, RGD-G3.5 was not toxic, and showed a similar ability in cell adhesion inhibition to free RGD at 2 h. In this fibroblast adhesion study, those rounded cells were not counted as adherent cells although they were attached to the surface at 2 h. We suspected that those initially rounded cells started to spread and proliferate within 96 hours as there was no significant difference in adherent cell density of those cells treated with free RGD, RGD-G3.5, or RGD-G4.0 when measured at 96 h.

The inhibited fibroblast adhesion to TCPS in the presence of RGD suspension was not well understood. However, as hydrophilic and ionic interaction between fibroblast and TCPS is essential for cell adhesion on TCPS, we believe that the binding of RGD clusters to the fibroblast via integrin receptors may lead to the decreased hydrophilic and ionic interaction between fibroblast and TCPS, thus disrupting cell adhesion. In addition, fibroblasts can secret adhesive fibronectin proteins in a serum-free medium (Grinnell and Feld 1979). Sufficient amounts of secreted fibronectin assist fibroblasts with attachment and spreading on the substrate (Grinnell and Feld 1979). It is envisioned that once the RGD clusters were introduced into the fibroblast suspension, the clustered RGD peptides would compete with the secreted fibronectin proteins in integrin-binding, resulting in competitive inhibition of integrin-mediated fibroblast adhesion to the TCPS substrate.

This work shows that anionic G3.5 PAMAM dendrimer can be used to construct dendritic RGD clusters with a similar ability in cell adhesion inhibition to free RGD. Once RGD peptides are clustered on the dendrimer surface, the number of available RGD tripeptides from the dendritic cluster for binding with cell membrane receptors may be reduced since only a portion of RGD peptides on the dendrimer surface can interact with the cell as illustrated in Figure 8. Therefore, high peptide loading degree of dendritic RGD clusters will not be necessary if the conjugated RGD tripeptides are not fully utilized for cell membrane binding. The marginal use of the conjugated RGD tripeptides on the dendrimer surface can be used to explain why the dendritic RGD clusters only showed comparable cell adhesion inhibition as opposed to free RGD in this study. The preliminary results have rendered the possibility of using nanoscale dendritic RGD clusters for drug delivery and tissue engineering applications. For example, a few RGD-containing peptides have been shown to bind to specific cell lines for tumor treatment and gene therapy (Colin et al 1998; Harbottle et al 1998; Aoki et al 2001). Dendritic RGD clusters containing abundant surface groups can be further modified with therapeutic entities to build dendrimer-based targeted drug delivery systems. Such targeted drug delivery systems will recognize cells containing integrin-receptors and exert therapeutic effects locally. Moreover, dendritic RGD clusters can be covalently grafted to the substrate to promote cell adhesion as free RGD-bound surface. Further functionalization of dendritic RGD clusters

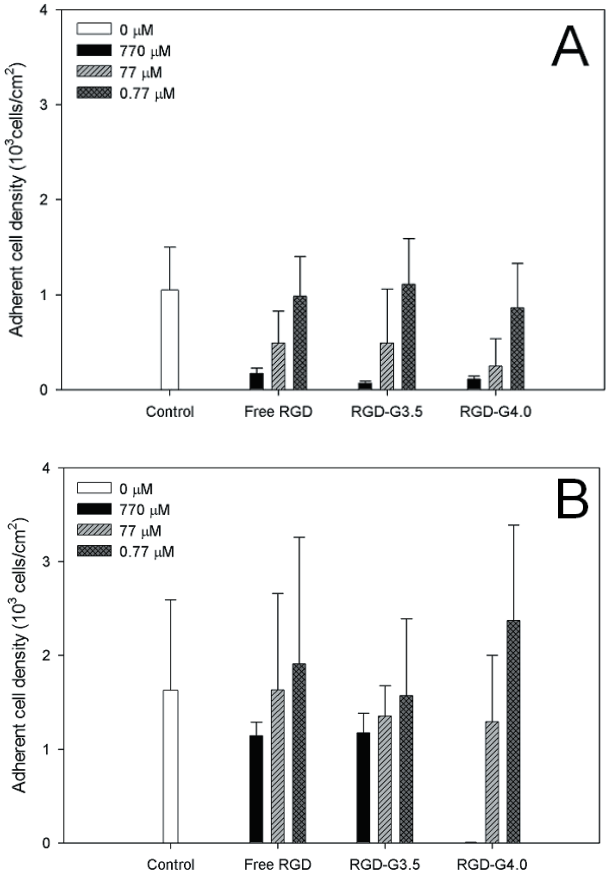

Figure 6 Adherent fibroblast density at 2 h (A) and 96 h (B) after 2 h-treatment with RGD peptides.
Abbreviation: RGD, arginine-glycine-aspartate.

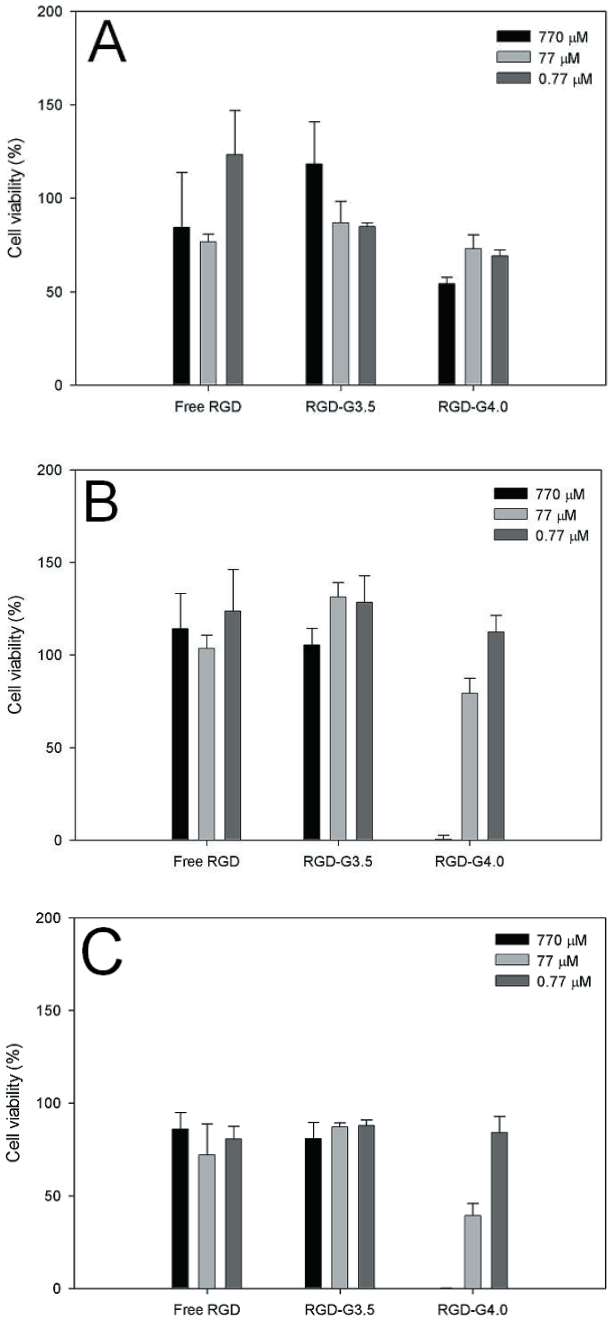

Figure 7 Viability of fibroblasts at 2 h (A), 24 h (B), and 96 h (C) after 2 h-treatment with RGD peptides.
Abbreviation: RGD, arginine-glycine-aspartate.

on the substrate will create unparalleled opportunities to develop highly adaptable and multifunctional substrates for tissue engineering applications. Future study will be focused on the impact of structural variation of dendritic RGD clusters on cellular responses and exploration of their potential drug delivery and tissue engineering applications.

Conclusions

Nanoscale dendritic RGD clusters were synthesized based on anionic G3.5 and cationic G4.0 PAMAM dendrimers. Biofunctionalized dendrimer structures were found highly dependent on the generation and the extent of peptide modification (ie, number of peptide per PAMAM). Anionic G3.5-based dendritic RGD clusters in suspension have shown no negative effect on fibroblast viability and a concentration-dependent effect on lowering cell adhesion to TCPS as that of free RGD. A concentration-dependent effect on cell viability and adhesion was also observed for cationic G4.0-based RGD at lower but not at high concentrations.

Acknowledgments

Hu Yang acknowledges the new faculty startup support from the Department of Biomedical Engineering at Virginia Commonwealth University. The authors thank the W. M. Keck Laboratory for Biological Imaging of the University of Wisconsin-Madison and Mr. Lance Rodenkirch for the assistance with confocal imaging. This work was supported by an NIH Grant (HL-077825).

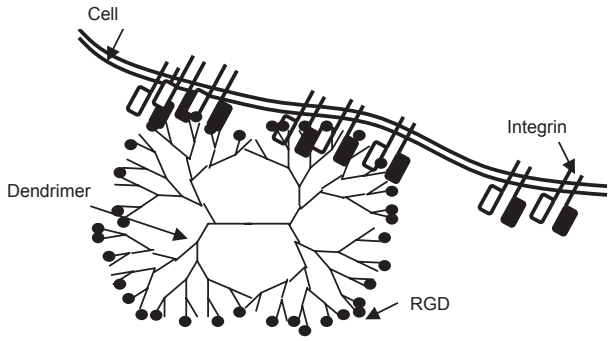

Figure 8 Schematic illustration of a nanoscale dendritic RGD cluster binding with integrin receptors.
Abbreviation: RGD, arginine-glycine-aspartate

References

Aoki Y, Hosaka S, Kawa S, et al. 2001. Potential tumor-targeting peptide vector of histidylated oligolysine conjugated to a tumor-homing RGD motif. *Cancer Gene Ther*, 8:783–7.

Bielinska A, Eichman JD, Lee I, et al. 2002. Imaging {Au0-PAMAM} Gold-dendrimer nanocomposites in cells. *J Nanoparticle Res*, 4:395–403.

Bielinska AU, Yen A, Wu HL, et al. 2000. Application of membrane-based dendrimer/DNA complexes for solid phase transfection in vitro and in vivo. *Biomaterials*, 21:877–87.

Bosman AW, Janssen HM, Meijer EW. 1999. About dendrimers: structure, physical properties, and applications. *Chem Rev (Washington DC)*, 99:1665–88.

Burridge K, Fath K, Kelly T, et al. 1988. Focal adhesions: transmembrane junctions between the extracellular matrix and the cytoskeleton. *Annu Rev Cell Biol*, 4:487–525.

Colin M, Harbottle RP, Knight A, et al. 1998. Liposomes enhance delivery and expression of an RGD-oligolysine gene transfer vector in human tracheal cells. *Gene Ther*, 5:1488–98.

Eichman JD, Bielinska AU, Kukowska-Latallo JF, et al. 2000. The use of PAMAM dendrimers in the efficient transfer of genetic material into cells. *Pharma Sci Technol Today*, 3:232–45.

Ginsberg MH, Du X, Plow EF. 1992. Inside-out integrin signalling. *Curr Opin Cell Biol*, 4:766–71.

Grinnell F, Feld MK. 1979. Initial adhesion of human fibroblasts in serum-free medium: possible role of secreted fibronectin. *Cell*, 17:117-29.

Harbottle RP, Cooper RG, Hart SL, et al. 1998. An RGD-oligolysine peptide: a prototype construct for integrin-mediated gene delivery. *Human Gene Ther*, 9:1037–47.

Hersel U, Dahmen C, Kessler H. 2003. RGD modified polymers: biomaterials for stimulated cell adhesion and beyond. *Biomaterials*, 24:4385–415.

Irvine DJ, Ruzette AV, Mayes AM, et al. 2001. Nanoscale clustering of RGD peptides at surfaces using comb polymers. 2. Surface segregation of comb polymers in polylactide. *Biomacromolecules*, 2:545–56.

Irvine DJ, Mayes AM, Griffith LG. 2001. Nanoscale clustering of RGD peptides at surfaces using Comb polymers. 1. Synthesis and characterization of Comb thin films. *Biomacromolecules*, 2:85–94.

Jevprasesphant R, Penny J, Jalal R, et al. 2003. The influence of surface modification on the cytotoxicity of PAMAM dendrimers. *Int J Pharm*, 252:263–6.

Jevprasesphant R, Penny J, Attwood D, et al. 2004. Transport of dendrimer nanocarriers through epithelial cells via the transcellular route. *J Control Release*, 97:259–67.

Kao WJ. 1999. Evaluation of protein-modulated macrophage behavior on biomaterials: designing biomimetic materials for cellular engineering. *Biomaterials*, 20:2213–21.

Khandare J, Kolhe P, Pillai O, et al. 2005. Synthesis, cellular transport, and activity of polyamidoamine dendrimer-methylprednisolone conjugates. *Bioconjug Chem*, 16:330–7.

Kobayashi H, Kawamoto S, Saga T, et al. 2001. Novel liver macromolecular MR contrast agent with a polypropylenimine diaminobutyl dendrimer core: Comparison to the vascular MR contrast agent with the polyamidoamine dendrimer core. *Magn Reson Med*, 46:795–802.

Kornberg LJ, Earp HS, Turner CE, et al. 1991. Signal transduction by integrins: increased protein tyrosine phosphorylation caused by clustering of beta 1 integrins. *Proc Natl Acad Sci U S A*, 88:8392–6.

Lai Johnathan C, Yuan C, Thomas James L. 2002. Single-cell measurements of polyamidoamine dendrimer binding. *Ann Biomed Engin*, 30:409–16.

Luo D, Haverstick K, Belcheva N, et al. 2002. Polyethylene glycol-conjugated PAMAM dendrimer for biocompatible, high-efficiency DNA delivery. *Macromolecules*, 35:3456–62.

Maheshwari G, Brown G, Lauffenburger DA, et al. 2000. Cell adhesion and motility depend on nanoscale RGD clustering. *J Cell Sci*, 113(Pt 10):1677–86.

Malik N, Wiwattanapatapee R, Klopsch R, et al. 2000. Dendrimers: Relationship between structure and biocompatibility in vitro, and preliminary studies on the biodistribution of 125I-labeled polyamidoamine dendrimers in vivo. *J Control Release*, 65:133–48.

Miyamoto S, Akiyama SK, Yamada KM. 1995. Synergistic roles for receptor occupancy and aggregation in integrin transmembrane function. *Science*, 267:883–5.

Miyamoto S, Teramoto H, Coso OA, et al. 1995. Integrin function: molecular hierarchies of cytoskeletal and signaling molecules. *J Cell Biol*, 131:791–805.

Poxon SW, Mitchell PM, Liang E, et al. 1996. Dendrimer delivery of oligonucleotide. *Drug Deliv*, 3:255–61.

Roberts JC, Bhalgat MK, Zera RT. 1996. Preliminary biological evaluation of polyamidoamine (PAMAM) starburst dendrimers. *J Biomed Mater Res*, 30:53–65.

Ruoslahti E, Pierschbacher MD. 1987. New perspectives in cell adhesion: RGD and integrins. *Science*, 238:491–7.

Shaw LM, Messier JM, Mercurio AM. 1990. The activation dependent adhesion of macrophages to laminin involves cytoskeletal anchoring and phosphorylation of the alpha 6 beta 1 integrin. *J Cell Biol*, 110:2167–74.

Shukla R, Thomas TP, Peters J, et al. 2005. Tumor angiogenic vasculature targeting with PAMAM dendrimer-RGD conjugates. *Chem Commun (Camb)*, 46:5739–41.

Tomalia DA, Baker H, Dewald J, et al. 1985. A new class of polymers: starburst-dendritic macromolecules. *Polym J (Tokyo)*, 17:117–32.

Yang H, Lopina ST. 2003. Penicillin V-conjugated PEG-PAMAM star polymers. *J Biomater Sci Polym Ed*, 14:1043–56.

Yang H, Morris JJ, Lopina ST. 2004. Polyethylene glycol-polyamidoamine dendritic micelle as solubility enhancer and the effect of the length of polyethylene glycol arms on the solubility of pyrene in water. *J Colloid Interface Sci*, 273:148–54.

Yang H, Lopina ST. 2005. Extended release of a novel antidepressant, venlafaxine, based on anionic polyamidoamine dendrimers and poly(ethylene glycol)-containing semi-interpenetrating networks. *J Biomed Mater Res*, 72A:107–14.

Yang H, Kao WJ. 2006. Dendrimers for pharmaceutical and biomedical applications. *J Biomater Sci Polym Ed*, 17:3–19.

Yang H, Lopina ST. 2006. In vitro enzymatic stability of dendritic peptides. *J Biomed Mater Res*, *Part A*, 76A:398–407.